

Identification of biomarkers for radiation-induced coronary heart disease in breast cancer patients

X.L. Huang, Z. Cai, Y. Xu*

Cardiac Intensive Care Unit (CCU), West China Hospital of Sichuan University, Chengdu, Sichuan, China

ABSTRACT

► Original article

***Corresponding author:**

Ying Xu, M.D.,

E-mail: 1419850448@qq.com

Received: October 2024

Final revised: December 2024

Accepted: December 2024

Int. J. Radiat. Res., April 2025; 23(2): 461-466

DOI: [10.61186/ijrr.23.2.28](https://doi.org/10.61186/ijrr.23.2.28)

Keywords: DNA, Hemoglobin A2, radiation-induced coronary heart disease, radiotherapy, single-cell RNA sequencing.

Background: This study aims to identify biomarkers associated with radiation-induced coronary heart disease (RICH) in breast cancer patients by integrating bioinformatics approaches with single-cell sequencing data, providing potential therapeutic targets for RICH treatment. **Materials and Methods:** Gene expression profiles associated with coronary heart disease were sourced from the Gene Expression Omnibus (GEO) database, and GEO2R was utilized to identify differentially expressed genes. Whole-genome sequencing and clinical data of breast cancer patients were obtained from The Cancer Genome Atlas (TCGA) database. Gene expression levels were analyzed using the 'Limma' package to compare radiation-exposed and non-exposed groups. Biological functional enrichment analysis was conducted using Gene Ontology (GO) and the Kyoto Encyclopedia of Genes and Genomes (KEGG). The intersection of TCGA and GEO identified key genes. Further analyses of these key genes in breast cancer patients were conducted using the GEPIA, Kaplan-Meier Plotter websites, and single-cell sequencing results. **Results:** The intersection of datasets from breast cancer and coronary heart disease revealed Hemoglobin A2(HBA2) as a key gene associated with RICH. HBA2 exhibited statistically significant differences in mRNA expression levels between breast cancer and normal tissues ($P<0.05$). Kaplan-Meier Plotter analysis revealed a significant prognostic difference between breast cancer patients with varying HBA2 expression levels ($P=0.005$). HBA2 exhibited significant expression levels in CD8+ T cells. **Conclusion:** HBA2 could be a biomarker and therapeutic target for RICH, offering new perspectives for clinical management of RICH patients.

INTRODUCTION

Radiotherapy (RT) is a widely used and effective treatment modality in breast cancer management, primarily aimed at reducing local recurrence and improving overall survival rates. Radiation therapy (RT) can increase the risk of cardiac complications, such as heart failure, coronary artery disease, and myocardial infarction, especially in patients with left-sided breast cancer (1-3). Coronary artery disease, a form of cardiovascular disease, ranks as the second leading cause of death among breast cancer patients treated with radiotherapy. The pathogenesis of radiation-induced coronary heart disease (RICH) is complex, involving multiple factors such as inflammation, fibrosis, vascular injury, and endothelial dysfunction (4). The impact of RT on the heart is influenced by various factors, including the radiation dose, treatment techniques, and individual risk factors of the patient. Studies have shown that for every 10 Gy increase in radiation dose to the heart, the risk of coronary artery disease and heart failure significantly rises (5). Deep inspiration breath-hold (DIBH) techniques significantly decrease heart radiation exposure, reducing cardiac damage risk (6, 7). Modern radiotherapy technologies, including intensity-modulated radiotherapy (IMRT)

and image-guided radiotherapy (IGRT), have shown potential in effectively reducing cardiac radiation exposure (8, 9). RICH may manifest years or even decades after treatment, significantly affecting the patient's quality of life and survival rate. Strengthening radiotherapy management, controlling radiation doses, administering preventive medications, and controlling hypertension early have all been proven to help reduce the risk of RICH (10-12). Screening for RICH biomarkers facilitates early detection of cardiac damage and enhances long-term quality of life in breast cancer patients (13, 14).

There is currently no consensus regarding biomarkers for RICH. Integrating the Cancer Genome Atlas (TCGA) and Gene Expression Omnibus (GEO) databases for bioinformatic analysis facilitates the identification of key hub genes essential for cancer progression and prognosis (15, 16). Research indicates that radiation-induced cardiovascular damage is frequently associated with endothelial cell injury and increased local inflammation, with specific intersecting genes potentially playing crucial roles in these processes. Moreover, the use of bioinformatics tools to analyze these datasets can deepen our understanding of the molecular mechanisms behind various diseases, revealing potential therapeutic targets and prognostic biomarkers (17, 18). Researchers

can validate the clinical significance of these biomarkers by utilizing protein-protein interaction (PPI) network and survival analyses (19, 20). This pioneering study examines the biological roles of differentially expressed genes in breast cancer patients undergoing radiotherapy compared to those not receiving it, as well as in coronary artery disease. It also proposes preliminary hypotheses on key genes and the pathogenesis of RICHID based on existing literature. This will provide theoretical support for the future development of novel molecular targeted interventions.

MATERIALS AND METHODS

Data collection and processing

The mRNA expression profiles, clinical-pathological features, and prognostic factors of breast invasive carcinoma samples with radiotherapy information were obtained from the TCGA database (<https://portal.gdc.cancer.gov/>). Data in TPM format were $\log_2(\text{TPM} + 1)$ normalized after extraction. A total of 165 breast cancer samples, comprising 73 treated with radiotherapy and 92 untreated, were included for analysis after ensuring the availability of both RNA-seq data and clinical information. Additionally, datasets related to coronary heart disease were sourced from the GEO database in MINiML format. For datasets that had not undergone normalization, a \log_2 transformation was uniformly applied. Non-standardized datasets were standardized using the normalize.Q function from the preprocess Core package in R, and batch effects were removed with the removeBatchEffect function from the limma package in R software (*R* software, version 4.0.3, Auckland, New Zealand).

Differential gene acquisition

We utilized the Limma package (version 3.40.2) in R software (*R* software, version 4.0.3, Auckland, New Zealand) to analyze differential mRNA expression in the TCGA and GEO datasets. Adjusted P-values were evaluated to mitigate false-positive outcomes in TCGA and GTEx datasets. Differentially expressed mRNA was identified using a threshold of an adjusted P-value below 0.05 and a $\log_2(\text{fold change})$ exceeding ± 1.3 .

GO Enrichment and KEGG Pathway Analysis

The DAVID (the Database for Annotation, Visualization and Integrated Discovery, <https://david.ncifcrf.gov/home.jsp>) online tool (<https://david.ncifcrf.gov/home.jsp>) was employed for functional annotation of differentially expressed genes (DEGs) using Gene Ontology (GO) to clarify their molecular functions, biological processes, and cellular components. Additionally, signaling pathways were visualized using the Kyoto

Encyclopedia of Genes and Genomes (KEGG) pathway analysis.

Hub gene expression and prognostic analysis

The GEPIA (Gene Expression Profiling Interactive Analysis) website was employed to compare the expression levels of key hub genes in breast cancer tissues versus normal tissues, with a significance threshold of $P \leq 0.05$. Additionally, the Kaplan-Meier Plotter online database (<https://www.kmplot.com/>) was employed to analyze the prognostic status of hub genes using receiver operating characteristic (ROC) curves, with a follow-up period of six months.

Gene expression analysis

We downloaded single-cell data in .h5 format, containing 45,000 immune cells from eight breast cancer cases, along with annotation results from Tumor Immune Single-cell Hub (TISCH) database. The R packages *MAESTRO* and *Seurat* were utilized for single-cell data processing and analysis, applying the t-distributed stochastic neighborhood embedding (t-SNE) method for cellular clustering.

RESULTS

Analysis of differential gene expression in the TCGA breast cancer dataset

A differential gene expression analysis was performed on the TCGA breast cancer dataset, comparing patients who underwent radiotherapy ($n=73$) to those who did not ($n=92$), using a significance threshold of $P < 0.05$. This analysis identified 34 upregulated genes (*C4orf19*, *SGCG*, *MT1M*, *DGAT2*, *SLC19A3*, *BAIAP2L2*, *MNX1*, *INSM1*, *AGT*, *DEPP1*, *ADAMTS1*, *IFI44L*, *SLC5A8*, *HBA2*, *TGFBR3*, *OSR1*, *CHI3L2*, *USP18*, *OLFM2*, *OPB2B*, *DOC2A*, *CHRD1L*, *ETV7*, *LEP*, *MX1*, *STC1*, *ASS1*, *NTN1*, *CST2*, *SAMD9L*, *ZNF750*, *IL6*, and *SERPINE2*) and 16 downregulated genes (*SPINK4*, *CLIC6*, *CABCOCO1*, *FLRT3*, *CAMK2B*, *MS4A8*, *IGFL2*, *HSPA2*, *ABHD2*, *OLFML3*, *SLC1A1*, *CEMIP*, *RAB31*, *MKX*, *DPYSL4*, and *RLN2*). Figure 1 displays a volcano plot (1A) and a heatmap (1B) depicting differential gene expression.

Figure 1 illustrates gene expression changes, where red dots indicate genes meeting both fold change (FC) and p-value thresholds, blue dots represent genes meeting only the p-value threshold, green dots denote genes meeting only the FC threshold, and grey dots signify genes that do not meet either threshold, indicating non-significant or minimal expression changes. (B) The heatmap displays sample clustering based on distribution from the outer to inner groups.)

GO and KEGG pathway analyses were conducted on the TCGA breast cancer dataset to examine differential gene expression. In the GO enrichment analysis, bar colors denote distinct GO term types, while bar lengths reflect the count of genes enriched

in each term. The 15 most significant results, each with $p < 0.05$, were presented. The up-regulated genes are primarily associated with pathways such as endocrine pancreas development, signaling receptor activator activity, sulfur compound binding, extrinsic components of the membrane, and collagen-containing extracellular matrix. Conversely, the down-regulated genes are mainly linked to pathways including positive regulation of calcium ion and endocytic vesicle. In the KEGG pathway enrichment results, different colors indicate the significance of functional enrichment, with larger values corresponding to smaller p-values. The size of the circles represents the number of enriched genes, with larger circles indicating a greater number of genes. The upregulated genes are predominantly associated with the pathway of hypertrophic cardiomyopathy, while the downregulated genes are primarily linked to lipid metabolism and atherosclerosis.

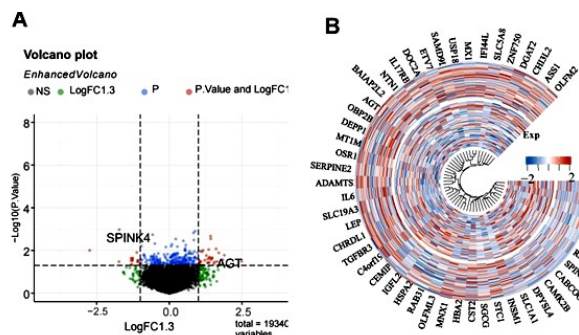


Figure 1. The study examines differential gene expression in breast cancer patients undergoing radiation therapy compared to those who do not. **(A)** The volcano plot illustrates gene expression changes, where red dots indicate genes meeting both fold change (FC) and p-value thresholds, blue dots represent genes meeting only the p-value threshold, green dots denote genes meeting only the FC threshold, and grey dots signify genes that do not meet either threshold, indicating non-significant or minimal expression changes. **(B)** The heatmap displays sample clustering based on distribution from the outer to inner groups.

Differential gene and enrichment analysis of CHD in GEO

We selected GSE23561 (GPL10775, Coronary heart disease: n=6, control group: n=9) and GSE120774 (GPL6244, Coronary heart disease: n=17, control group: n=19) for differential gene queries. Differential up-regulated genes included 24 and down-regulated genes included 83 in the coronary heart disease group (n=23) and normal group (n=28). The differentially expressed gene profiles are shown in volcano (figure 2A) and heatmap (figure 2B). GO-enriched pathways were mainly endocytic vesicle, organic acid binding, blood microparticle and detection of chemical stimulus involved, KEGG-enriched pathways were mainly Viral myocarditis, Olfactory transduction and Rap1

signaling pathway.

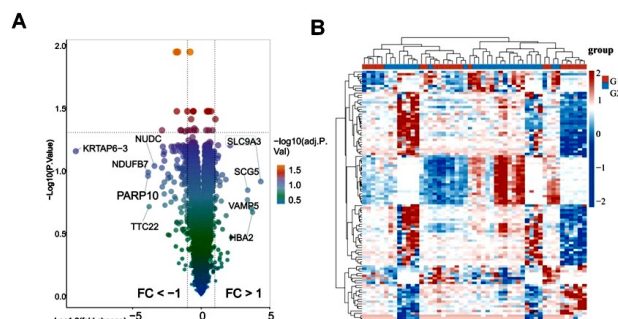


Figure 2. Differential gene expression in the CHD dataset in GEO **(A)**, volcano plot; **(B)**, heat map).

Expression and prognostic analysis of intersecting genes

Hemoglobin A2 (HBA2) was the intersecting gene between the TCGA dataset and the GEO dataset. Analysis of HBA2 expression in breast cancer cancers and normal tissues using the GEPIA website (figure 3A) revealed a *statistical difference* (*represents $p < 0.05$) in mRNA gene expression. Kaplan-Meier Plotter analysis revealed a significant prognostic difference in breast cancer patients based on HBA2 expression levels (HR=0.87, 95% CI 0.78-0.96, $P=0.005$) (figure 3B).

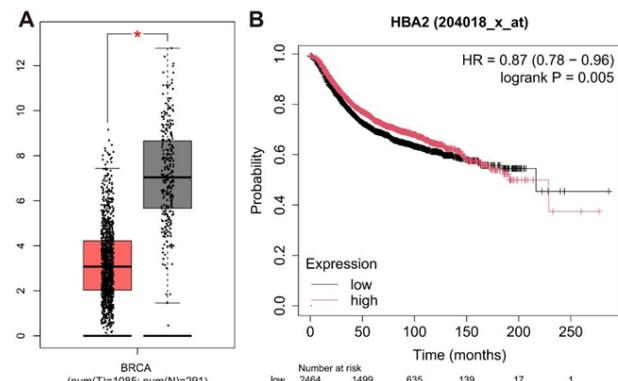


Figure 3. GEPIA differential expression profile of HBA2 and Kaplan-Meier Plot survival analysis **(A)**, GEPIA differential expression profile, **(B)**, HBA2 high and low expression in Kaplan-Meier Plotter for survival analysis of breast cancer patients).

HBA2 expression in cells from breast cancer patients

Based on single-cell data from eight breast cancer samples totaling 45,000 immune cells, we found significant differences in the expression of the *HBA2* gene in different cell types (figure 4A, figure 4B). The high expression of the gene in CD8T cells suggests that *HBA2* may play an important biological function in this cell type, which informs further studies on the role of *HBA2* in immune-related cells. Meanwhile, the moderate expression levels in fibroblasts and mast cells may also suggest a specific role for the gene in these cell types (figure 4C).

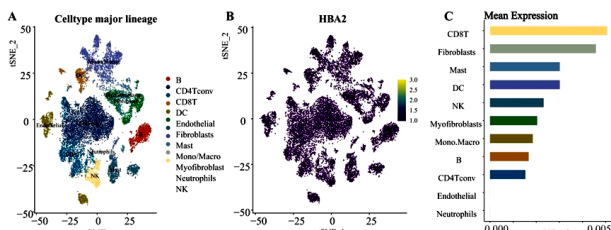


Figure 4. The expression of *HBA2* in breast cancer patient cells is illustrated through various visualizations. **A.** A single-cell clustering t-SNE plot where distinct cell types are indicated by different colors; **B.** A t-SNE plot showing the distribution of selected gene expressions across different cells, with color intensity reflecting expression levels-darker shades indicate lower expression, while brighter shades denote higher expression; **C.** A histogram depicting the abundance of selected genes in various cells).

DISCUSSION

RT is an important modality in the treatment of breast cancer, although it is gaining attention due to RICHD. By identifying differentially expressed genes associated with RICHD, we can better understand the mechanisms through which radiation therapy affects cardiac health in breast cancer patients, potentially providing biomarkers and therapeutic targets for clinical applications. Numerous studies employing bioinformatics have analyzed breast cancer gene expression profiles, identifying crucial genes associated with disease progression and prognosis (22). Additionally, in addressing radiation-induced cardiac injury, researchers are actively exploring different biomarkers in hopes of improving patient outcomes (23). Integrating data from the TCGA and GEO databases enables researchers to more comprehensively identify RICHD-associated genes, thus providing a theoretical basis for future clinical research and therapeutic strategies (24).

Our results indicate that, compared to breast cancer patients who did not undergo radiation therapy, those who did showed 34 upregulated genes and 16 downregulated genes. This finding highlights the influence of radiation therapy on the molecular profile of breast cancer, indicating that it may trigger specific gene expression alterations that enhance our understanding of treatment response and resistance mechanisms in patients (25). GO pathway enrichment analysis suggests these genes may play pivotal roles in endocrine system development, signal transduction, cell membrane structure and function, and the maintenance and remodeling of the extracellular matrix (ECM) (26-29). Dynamic changes in the ECM are closely associated with tissue repair and regeneration in various organs, including the heart, liver, and nervous system (27, 30). KEGG pathway enrichment analysis of the differentially expressed genes indicated links to hypertrophic cardiomyopathy (HCM) and lipid metabolism, where

disruptions in lipid homeostasis may worsen atherosclerosis and result in significant cardiovascular events (31).

Our findings identified *HBA2* as a key gene for RICHD. In breast cancer patients, coronary artery disease risk factors such as hypertension, diabetes, and hypercholesterolemia may be affected by *HBA2* gene variants (32). Other studies have shown that *HBA2* expression levels are associated with cardiac function changes, possibly affecting heart health indirectly by influencing oxygen transport in the blood (33). Thus, studying *HBA2* not only aids in understanding RICHD risk in breast cancer patients but may also provide a foundation for developing new therapeutic strategies. Our GEPIA analysis indicated a statistically significant difference in *HBA2* mRNA expression between cancerous and normal breast tissues. This finding aligns with other studies, suggesting that *HBA2* may play a vital role in breast cancer initiation and progression (34). Our Kaplan-Meier Plotter analysis revealed a significant prognostic difference in breast cancer patients based on *HBA2* expression levels, aligning with findings from other studies. Research by Sun *et al.* showed that high *HBA2* expression is associated with extended survival in breast cancer patients, whereas low expression correlates with a poorer prognosis (35). Moreover, *HBA2* expression may relate to tumor stage, grade, and other clinicopathological characteristics, further emphasizing its potential as a biomarker (36). Therefore, *HBA2* expression could serve as a predictive factor for breast cancer prognosis and offer new insights for individualized treatment (37). Some studies have also identified other key targets, e.g., Cui *et al.* Ring finger protein 146 has been linked to the prognosis of breast cancer patients, necessitating further validation of these targets (38).

Single-cell data analysis showed high *HBA2* expression in CD8+ T cells of breast cancer patients, suggesting a strong connection to immune responses within the tumor microenvironment. CD8+ T cells are key effectors of antitumor immunity, and their enhanced function is closely linked to tumor prognosis. Studies have indicated that CD8+ T cell activity is associated with tumor cell characteristics, cytokines in the microenvironment, and the expression levels of tumor-associated antigens (39). In breast cancer, CD8+ T cell infiltration generally correlates positively with patient survival, particularly in HER2-positive and triple-negative breast cancer cases (40). High *HBA2* expression may reflect adaptive changes in CD8+ T cells within the tumor microenvironment, potentially linked to tumor cell metabolic states and immune evasion mechanisms. Research has shown that tumor cells can suppress CD8+ T cell function by altering metabolic pathways, thereby promoting tumor growth and metastasis (41). Additionally, *HBA2* expression might correlate with immunosuppressive

factors, such as PD-L1 expression, which help tumor cells evade immune surveillance by inhibiting CD8+ T cell activity⁽⁴²⁾. Therefore, *HBA2*'s high expression in CD8+ T cells may not only indicate changes in the tumor micro environment but also serve as a potential target for breast cancer immunotherapy. Future studies should investigate *HBA2*'s specific role in CD8+ T cell function and its potential applications in breast cancer immunotherapy⁽⁴³⁾.

This study has certain limitations. First, heterogeneity and potential bias in the database data sources could impact the reliability and general applicability of our findings, especially with smaller sample sizes. Additionally, limited clinical information in many data sources restricts deeper analysis of the relationship between gene expression, disease severity, and patient prognosis. Data insufficiency, version inconsistencies, and update frequency within databases may further reduce result reproducibility. While tools like GEPPIA offer convenience, their algorithmic and parameter limitations may impact accuracy. Finally, since the identified genes in database analyses indicate associations rather than causal relationships, further biological experiments are necessary to verify the actual role of these key genes in disease.

CONCLUSION

The elevated expression of *HBA2* in CD8+ T cells indicates its potential significance in immune responses and RICHD development, offering a novel avenue for precision treatment of RICHD. Future research could further explore the specific mechanisms of *HBA2* in the pathogenesis of RICHD and validate its clinical application potential as a therapeutic target, offering more effective personalized treatment options for RICHD patients.

ACKNOWLEDGEMENTS

The authors would like to express their sincere thanks to all the researchers and organizations that contributed to this study.

Conflicts of Interest: All authors unanimously declare that there is no conflict of interest in this study.

Funding: This study was supported by no funding.

Ethical consideration: Not applicable.

Authors' contribution: X-L.H. and Z.C. conceived the study and designed the research. X-L.H. was responsible for the data analysis and interpretation, including the bioinformatics analysis using GEO, TCGA, and KEGG databases, as well as the identification of key genes. Z.C. contributed to the statistical analysis and the validation of the findings through Kaplan-Meier survival analysis and further bioinformatics tools. Y.X. provided guidance on the study design, assisted with the interpretation of the

results, and supervised the overall research process. All authors participated in writing, revising, and approving the final manuscript for submission.

REFERENCES

1. Song J, Tang T, Caudrelier JM, et al. (2021) Dose-sparing effect of deep inspiration breath hold technique on coronary artery and left ventricle segments in treatment of breast cancer. *Radiat Oncol*, **154**: 101-109.
2. Pan L, Lei D, Wang W, et al. (2020) Heart dose linked with cardiac events and overall survival in lung cancer radiotherapy: A meta-analysis. *Medicine (Baltimore)*, **99**: e21964.
3. Pedersen PH, Vergari C, Tran A, et al. (2019) A Nano-dose protocol for Cobb angle assessment in children with scoliosis: results of a phantom-based and clinically validated study. *Clin Spine Surg*, **32**: E340-e345.
4. Yang EH, Marmagkiolis K, Balanescu DV, et al. (2021) Radiation-induced vascular disease-a state-of-the-art review. *Front Cardiovasc Med*, **8**: 652761.
5. Bates JE, Rancati T, Keshavarz H, et al. (2024) Cardiac disease in childhood cancer survivors treated with radiation therapy: A PENTEC Comprehensive review. *Int J Radiat Oncol Biol Phys*, **119**: 522-532.
6. Leung HW, Chan AL, Muo CH (2016) Late cardiac morbidity of adjuvant radiotherapy for early breast cancer - A population-based study. *J Cardiol*, **67**: 567-571.
7. Marks LB, Zagar TM, Kaidar-Person O (2017) Reassessing the time course for radiation-induced cardiac mortality in patients with breast cancer. *Int J Radiat Oncol Biol Phys*, **97**: 303-305.
8. Jacob S, Pathak A, Franck D, et al. (2016) Early detection and prediction of cardiotoxicity after radiation therapy for breast cancer: the BACCARAT prospective cohort study. *Radiat Oncol*, **11**: 54.
9. Riou O, Bourgier C, Fenoglietto P, et al. (2015) Does nodal irradiation (clavicular and internal mammary chains) increase the toxicity of adjuvant breast radiotherapy? *Cancer Radiother*, **19**: 261-264.
10. Cuomo JR, Sharma GK, Conger PD, et al. (2016) Novel concepts in radiation-induced cardiovascular disease. *World Journal of Cardiology*, **8**: 504-519.
11. Banaei A, Hashemi B, Bakhshandeh M (2022) Estimating cancer risks due to whole lungs low dose radiotherapy with different techniques for treating COVID-19 pneumonia. *Radiation Oncology*, **17**: 10.
12. van Nimwegen FA, Schaapveld M, Cutler DJ, et al. (2016) Radiation dose-response relationship for risk of coronary heart disease in survivors of Hodgkin lymphoma. *J Clin Oncol*, **34**: 235-243.
13. Henson KE, McGale P, Darby SC, et al. (2020) Cardiac mortality after radiotherapy, chemotherapy and endocrine therapy for breast cancer: Cohort study of 2 million women from 57 cancer registries in 22 countries. *Int J Cancer*, **147**: 1437-1449.
14. Kim L, Locco EC, Sanchez R, et al. (2020) Contemporary understandings of cardiovascular disease after cancer radiotherapy: a focus on ischemic heart disease. *Curr Cardiol Rep*, **22**: 151.
15. Wan Y, Zhang X, Leng H, et al. (2020) Identifying hub genes of papillary thyroid carcinoma in the TCGA and GEO database using bioinformatics analysis. *PeerJ*, **8**: e9120.
16. Song D, Tian J, Hu Y, et al. (2020) Identification of biomarkers associated with diagnosis and prognosis of gastroesophageal junction adenocarcinoma-a study based on integrated bioinformatics analysis in GEO and TCGA database. *Medicine (Baltimore)*, **99**: e23605.
17. Zeng L, Fan X, Wang X, et al. (2019) Bioinformatics analysis based on multiple databases identifies hub genes associated with hepatocellular carcinoma. *Curr Genomics*, **20**: 349-361.
18. Xiao H, Wang K, Li D, et al. (2021) Evaluation of FGFR1 as a diagnostic biomarker for ovarian cancer using TCGA and GEO datasets. *PeerJ*, **9**: e10817.
19. You Y, Ru X, Lei W, et al. (2020) Developing the novel bioinformatics algorithms to systematically investigate the connections among survival time, key genes and proteins for Glioblastoma multiforme. *BMC Bioinformatics*, **21**: 383.
20. Xu Y, Wu G, Li J, et al. (2020) Screening and identification of key biomarkers for bladder cancer: A study based on TCGA and GEO data. *Biomed Res Int*, **2020**: 8283401.
21. Azizi E, Carr AJ, Plitas G, et al. (2018) Single-cell map of diverse immune phenotypes in the breast tumor microenvironment. *Cell*, **174**: 1293-1308.e1236.
22. Mo L, Liu J, Yang Z, et al. (2020) DNAB4 identified as a potential

breast cancer marker: evidence from bioinformatics analysis and basic experiments. *Gland Surg*, **9**: 1955-1972.

23. Xue JM, Liu Y, Wan LH, et al. (2020) Comprehensive analysis of differential gene expression to identify common gene signatures in multiple cancers. *Med Sci Monit*, **26**: e919953.

24. Liu S, Liu X, Wu J, et al. (2020) Identification of candidate biomarkers correlated with the pathogenesis and prognosis of breast cancer via integrated bioinformatics analysis. *Medicine (Baltimore)*, **99**: e23153.

25. Dan WC, Guo XY, Zhang GZ, et al. (2023) Integrative analyses of radiation-related genes and biomarkers associated with breast cancer. *Eur Rev Med Pharmacol Sci*, **27**: 256-274.

26. Chen J, Hou C, Wang P, et al. (2019) Grade II/III glioma microenvironment mining and its prognostic merit. *World Neurosurg*, **132**: e76-e88.

27. Frangogiannis NG (2017) The extracellular matrix in myocardial injury, repair, and remodeling. *J Clin Invest*, **127**: 1600-1612.

28. Karsdal MA, Manon-Jensen T, Genovese F, et al. (2015) Novel insights into the function and dynamics of extracellular matrix in liver fibrosis. *Am J Physiol Gastrointest Liver Physiol*, **308**: G807-830.

29. Oskarsson T (2013) Extracellular matrix components in breast cancer progression and metastasis. *Breast*, **22 (Suppl 2)**: S66-72.

30. Sun Y, Zou J, Ouyang W, et al. (2020) Identification of PDE7B as a potential core gene involved in the metastasis of clear cell renal cell carcinoma. *Cancer Manag Res*, **12**: 5701-5712.

31. Hou C, Fei S, Jia F (2024) Necroptosis and immune infiltration in hypertrophic cardiomyopathy: novel insights from bioinformatics analyses. *Front Cardiovasc Med*, **11**: 1293786.

32. Bielinski SJ, Berardi C, Decker PA, et al. (2017) Hepatocyte growth factor demonstrates racial heterogeneity as a biomarker for coronary heart disease. *Heart*, **103**: 1185-1193.

33. Dong Y, Chen H, Gao J, et al. (2019) Molecular machinery and interplay of apoptosis and autophagy in coronary heart disease. *J Mol Cell Cardiol*, **136**: 27-41.

34. Chen B, Tang H, Chen X, et al. (2019) Transcriptomic analyses identify key differentially expressed genes and clinical outcomes between triple-negative and non-triple-negative breast cancer. *Cancer Manag Res*, **11**: 179-190.

35. Sun X, Sun Z, Zhu Z, et al. (2014) Clinicopathological significance and prognostic value of lactate dehydrogenase A expression in gastric cancer patients. *PLoS One*, **9**: e91068.

36. Yang L, Yu J, Tao L, et al. (2022) Cuproptosis-related lncRNAs are biomarkers of prognosis and immune microenvironment in head and neck squamous cell carcinoma. *Front Genet*, **13**: 947551.

37. Tian C, Zhou S, Yi C (2018) High NUP43 expression might independently predict poor overall survival in luminal A and in HER2+ breast cancer. *Future Oncol*, **14**: 1431-1442.

38. Li X, Gao Y, Kou C, et al. (2024) Association of the RNF146 rs2180341 single nucleotide polymorphism with breast cancer susceptibility and prognosis in northern Chinese population. *Indian Journal of Pharmaceutical Sciences*, **86**: 8.

39. Umemura S, Shirane M, Takekoshi S, et al. (2010) High expression of thymidine phosphorylase in basal-like breast cancers: Stromal expression in EGFR- and/or CK5/6-positive breast cancers. *Oncol Lett*, **1**: 261-266.

40. Gates JD, Clifton GT, Benavides LC, et al. (2010) Circulating regulatory T cells (CD4+CD25+FOXP3+) decrease in breast cancer patients after vaccination with a modified MHC class II HER2/neu (AE37) peptide. *Vaccine*, **28**: 7476-7482.

41. Greene LI, Bruno TC, Christenson JL, et al. (2019) A role for tryptophan-2,3-dioxygenase in CD8 T-cell suppression and evidence of tryptophan catabolism in breast cancer patient plasma. *Mol Cancer Res*, **17**: 131-139.

42. Andreata F, Iannaccone M (2024) The hidden strength of CD8(+) T cells in chronic hepatitis B. *Nat Immunol*, **25**, 1515-1516.

43. Kuznetsova M, Lopatnikova J, Shevchenko J, et al. (2019) Cytotoxic activity and memory T cell subset distribution of in vitro-stimulated CD8(+) T cells specific for HER2/neu Epitopes. *Front Immunol*, **10**: 1017.